Volume 51 | Number 48 | 18 June 2015 | Pages 9747–9908

ChemComm

Chemical Communications

www.rsc.org/chemcomm

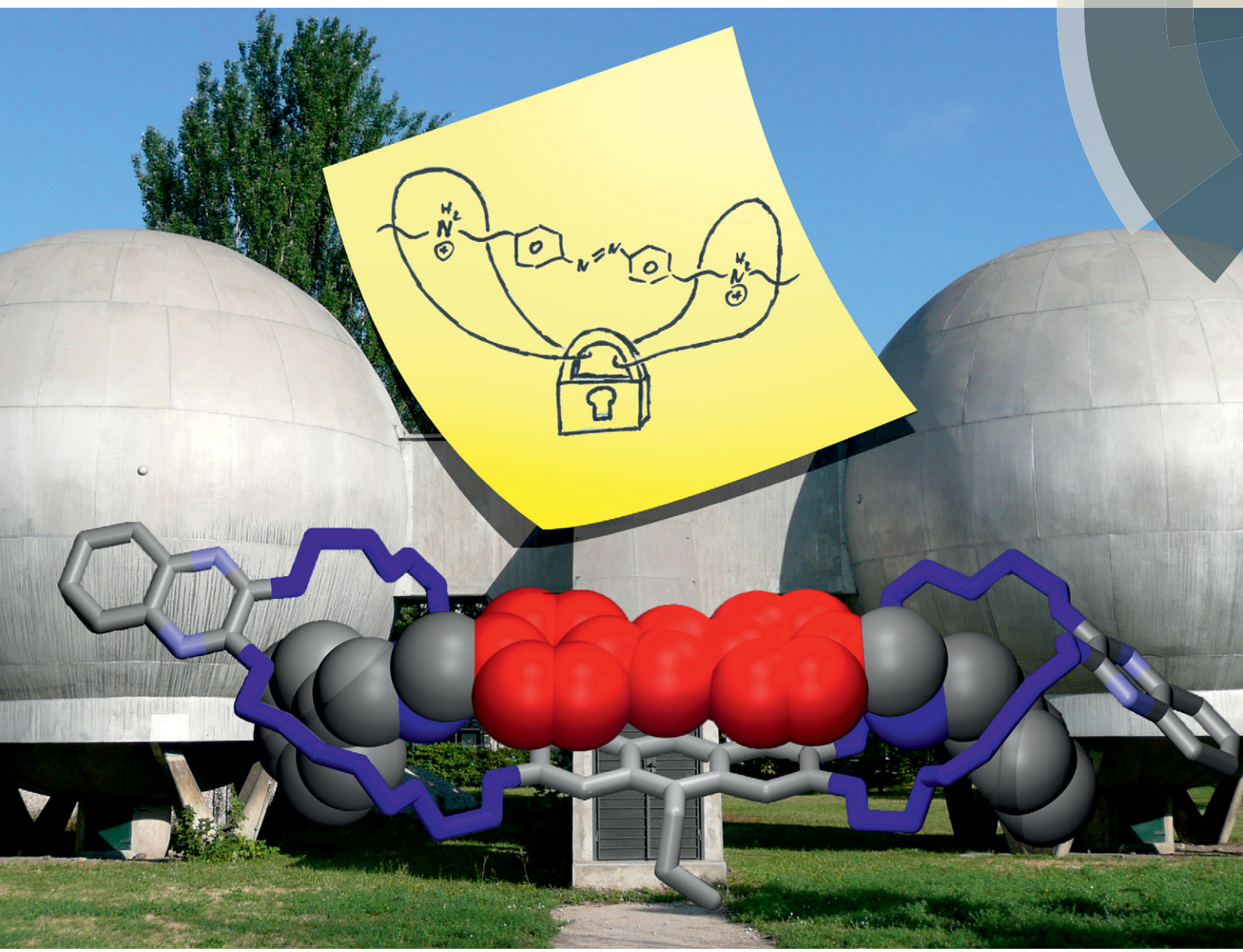

ISSN 1359-7345

ROYAL SOCIETY OF CHEMISTRY

COMMUNICATION

Beate Paulus, Christoph A. Schalley, Stefan Hecht *et al.*

Gating the photochromism of an azobenzene by strong host–guest interactions in a divalent pseudo[2]rotaxane

ChemComm

COMMUNICATION

View Article Online
View Journal | View Issue

Cite this: *Chem. Commun.*, 2015, **51**, 9777

Received 4th April 2015,
Accepted 23rd April 2015

DOI: 10.1039/c5cc02811f

www.rsc.org/chemcomm

Gating the photochromism of an azobenzene by strong host–guest interactions in a divalent pseudo[2]rotaxane†

Mirko Lohse,[a] Karol Nowosinski,[b] Nora L. Traulsen,[b] Andreas J. Achazi,[b] Larissa K. S. von Krbek,[b] Beate Paulus,*[b] Christoph A. Schalley*[b] and Stefan Hecht*[a]

The ability of an *E*-configured azobenzene guest to undergo photoisomerisation is controlled by the presence of a complementary host. Addition of base/acid allowed for a weakening/strengthening of the interactions in the divalent pseudo[2]rotaxane complex and hence could switch on/off photochromic activity.

Photochromism, the reversible switching of a molecule between two states by light, provides an excellent tool for the development of smart materials by gaining remote control over their properties *via* an external stimulus.[1] Being able to turn on and off the ability of a photoswitch to isomerise, so-called "gated photochromism", is desirable to implement responsiveness to multiple stimuli[2] and has primarily been achieved by acid–base reactions or coordination of (transition) metal ions.[3] In addition, specific host–guest interactions involving one isomer of the photoswitch selectively could in principle also be employed to gate the switching process and in turn provide photocontrol over the association process. The underlying binding event should be readily modulated by large structural changes in either the host or guest. Therefore, it seems reasonable to utilise a photoswitch, which undergoes a light-induced *E*–*Z* double bond isomerisation. In this context, azobenzene can be considered as the "drosophila" in the field. Its significant structural changes upon *E*–*Z* photoisomerisation have been used to modulate microscopic[4] and even macroscopic[5] property changes, which have been exploited in various areas from chemistry[6] over material science[1,5,7] to biology[8] and potentially pharmacology.[9] Whereas authors typically care about the influence of azobenzene photoisomerisation on the resulting supramolecular structure,[10] much less attention has been paid to cases where the non-covalent interactions influence the azobenzene's photoswitchability.[11]

Here, we describe the first pseudo[2]rotaxane assembly involving a divalent crown ether host and a divalent photochromic azobenzene guest. By making or breaking of the host–guest complex we can either lock or unlock the *E*-isomer and thereby gate its photoisomerisation ability.

The key components of our host–guest system are photochromic axles **1** and **2**, carrying two terminal secondary ammonium-binding sites, which are based on azobenzene and stilbene, respectively (Fig. 1). The latter has been prepared in particular to access *Z*-**2** as a thermally stable, structural analogue of *Z*-**1**.[12] Based on the well-known and tuneable interaction between a secondary ammonium ion and a dibenzo-24-crown-8,[13] anthracene-spacered divalent crown ether **3**[14] was chosen as the complementary divalent host. In addition, monovalent ammonium guest **5** and monovalent crown ether **4** were prepared for comparison purposes.

Synthesis of the azobenzene axle **1** involves a straightforward linear sequence of reductive amination of 4-nitrobenzaldehyde with benzyl amine and BOC-protection, followed by reduction to the aniline derivative and oxidative dimerization. BOC-deprotection and protonation with NH_4PF_6 finally yields hexafluorophosphate salt *E*-**1**. Axles *E*-**2** and *Z*-**2** were derived from the corresponding (*E*)-[15] and (*Z*)-stilbene[16] dialdehydes *via* reductive amination and protonation. The synthesis and characterisation of host **3** have been described previously.[14] More information about the synthesis and compound characterisation is provided in the ESI.†

To investigate the host–guest interactions between guest *E*-**1** and host **3**, ^{1}H NMR spectroscopy experiments have been carried out. In an equimolar mixture, a new set of signals appears, which is related to complex *E*-**1**@**3** (Fig. 2 top, see also ESI†, Fig. S1 and S2). Whereas significant chemical upfield shifts were observed for the aromatic protons H_d ($\Delta\delta \approx 0.35$ ppm) and H_e ($\Delta\delta \approx 0.7$ ppm) of the azobenzene core of axle *E*-**1** due to their position atop the anthracene unit of host **3** indicating exclusive formation of doubly bound dimers. The benzylic protons H_b and H_c shifted downfield ($\Delta\delta \approx 0.5$ ppm) upon complexation. These large shifts can be explained by the location of the azobenzene protons above the

[a] *Department of Chemistry, Humboldt-Universität zu Berlin, Brook-Taylor-Str. 2, 12489 Berlin, Germany. E-mail: sh@chemie.hu-berlin.de; Fax: +49 (0)30 2093-6940; Tel: +49 (0)30 2093-7308*

[b] *Institut für Chemie und Biochemie, Freie Universität Berlin, Takustraße 3, 14195 Berlin, Germany. E-mail: b.paulus@fu-berlin.de, christoph@schalley-lab.de; Fax: +49 (0)30 838-55366; Tel: +49 (0)30 838-52639*

† Electronic supplementary information (ESI) available: Experimental procedures and characterisation data, ITC and photochemistry experiments. See DOI: 10.1039/c5cc02811f

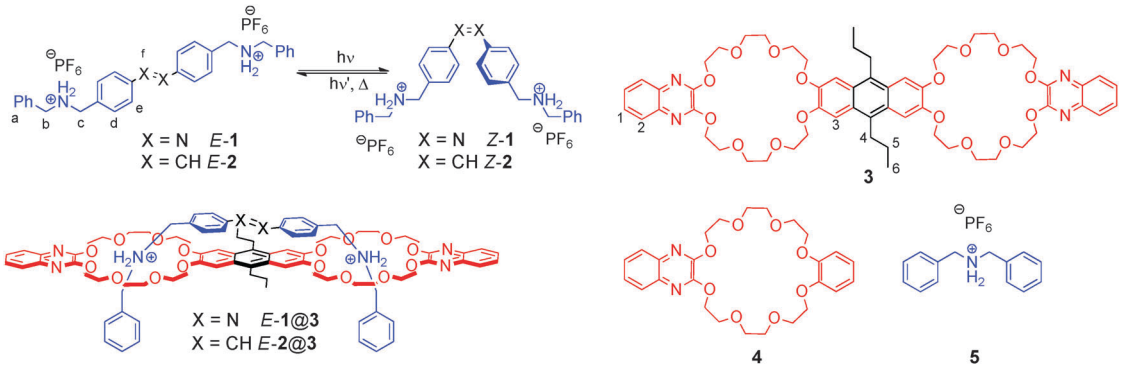

Fig. 1 Isomerization of divalent azobenzene and stilbene axles **1** and **2**, divalent host **3**, monovalent reference compounds **4** and **5**, as well as divalent pseudo[2]rotaxanes *E*-**1**@**3** and *E*-**2**@**3**.

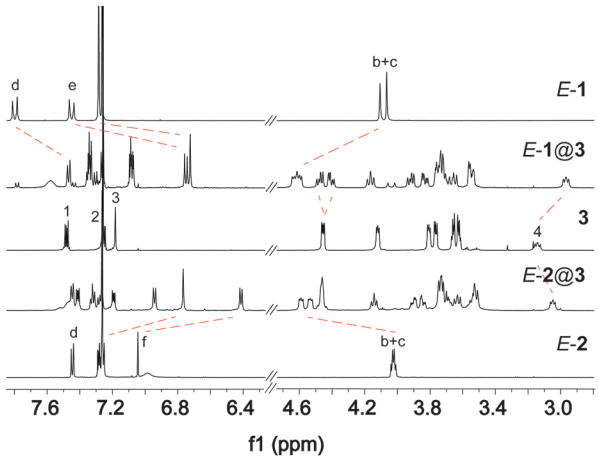

Fig. 2 ^{1}H NMR experiment of the complexation of azobenzene axle *E*-**1** (top) as well as *E*-**2** (bottom) to host **3** (500 MHz, $CDCl_3$: CD_3CN 2 : 1, 1.4 mM). The dashed lines indicate the shifting of selected protons upon formation of the complex.

anthracene core of host **3** on the one hand and the deshielding of the benzylic protons due to C–H···O hydrogen-bonding with the crown ether oxygen atoms as well as due to the aromatic ring current of the anthracene spacer, on the other. Note that the splitting of several peaks for crown ether methylene groups in the complex *E*-**1**@**3** is caused by the threading of the axle through the host, resulting in new sets of diastereotopic proton signals. EXSY NMR studies show that in the chosen solvent mixture ($CDCl_3$: CD_3CN = 2 : 1) there is no detectable exchange between the bound and free axle *E*-**1**, indicating that dethreading is slow. In addition, ESI mass spectrometry supports the formation of the complex *E*-**1**@**3** (see ESI†, Fig. S25).

Trying to elucidate the structure of the host–guest complex formed by the photoisomerised axle *Z*-**1** is practically impossible due to its thermal $Z \rightarrow E$ back isomerisation (note that the inevitably forming *E*-**1** binds to the host **3** much more strongly). Therefore, the isosteric stilbene axles *E*-**2** and *Z*-**2** have been studied. While ^{1}H NMR titration reveals formation of a stable 1 : 1 complex *E*-**2**@**3** (Fig. 2, bottom), the *Z*-configured axle *Z*-**2** does not yield a well-defined complex upon addition of **3** (see ESI†, Fig. S27).

Table 1 Thermodynamic binding data of *E*-**1**@**3**, **5**@**4**, *E*-1@$\mathbf{4}_2$ and $\mathbf{5}_2$@**3** as obtained from ITC experiments ($CHCl_3$: CH_3CN = 2.2 : 1, 298 K)

Complex	K_a [M^{-1}]		ΔG [kJ mol^{-1}]	ΔH^* [kJ mol^{-1}]	$T\Delta S^{*a}$ [kJ mol^{-1}]
E-**1**@**3**		$2 \times 10^5 \pm 2 \times 10^4$	−30.3 ± 0.2	−52.1	−21.9
5@**4**		1800 ± 200	−18.6 ± 0.2	−39.3	−20.6
E-**1**@$\mathbf{4}_2$	K_1	3100 ± 300	−19.9 ± 0.3	−27.6	−7.7
	K_2	870 ± 90	−16.8 ± 0.2	−35.0	−18.1
$\mathbf{5}_2$@**3**	K_1	3700 ± 400	−20.4 ± 0.2	−26.3	−5.9
	K_2	170 ± 20	−12.7 ± 0.3	−32.9	−20.2

[a] ΔH and ΔS values have larger errors than those of ΔG and should be regarded as estimate rather than precise values.

In order to investigate the association behaviour of the different axles with the host more thoroughly, a detailed thermodynamic analysis of the assembly was carried out involving isothermal titration calorimetry (ITC), which has proven very insightful for studying strongly bound pseudorotaxanes.[17] In contrast to similar pseudo[2]rotaxanes based on crown ether–ammonium interactions,[17] a very strong binding was observed for complex *E*-**1**@**3**, giving rise to an unusually high association constant of K_a = 200 000 M^{-1} (Table 1). This strong interaction demonstrates the perfect fit of axle *E*-**1** to host **3**. Additional secondary binding events, such as acceptor–donor type π,π-stacking of the electron-deficient azobenzene and the electron-rich anthracene cores,[18] together with the divalent complexation contribute to a large effective molarity (EM) value of 380 mM and a highly positive chelate cooperativity factor of $K_{mono} \times EM = 340 \gg 1$.[19] Additional ITC experiments to deduce the association constants of the stilbene-based complexes *E*-**2**@**3** and *Z*-**2**@**3** were not successful due to insufficient solubility of the axle components. However, in an insightful competition experiment monitored by ^{1}H NMR spectroscopy it could be shown that upon addition of *E*-**1** to an equimolar solution of *Z*-**2** and **3**, *E*-**1**@**3** was formed rapidly (see Fig. S30 in ESI†). This indicates that the association constant of *Z*-**2**@**3** containing the *Z*-configured (stilbene) axle has to be much lower than the one of the complex composed of the *E*-configured (azobenzene) axle. The association constants of the monovalent model complexes **5**@**4**, *E*-**1**@$\mathbf{4}_2$ and $\mathbf{5}_2$@**3** are all lower and in a similar range. Higher K_a values for the first binding step in case of *E*-**1**@$\mathbf{4}_2$ and $\mathbf{5}_2$@**3** compared to **5**@**4** are expected due to statistics. However, both show negative allosteric

interaction[19] with reduced K_a values for the second binding step and allosteric cooperativity factors $\alpha(E\text{-}\mathbf{1}@\mathbf{4}_2)$ = 0.8 and $\alpha(\mathbf{5}_2@\mathbf{3})$ = 0.2, which has been found before for similar systems.[17] We attribute the quite strong negative allosteric cooperativity of $\mathbf{5}_2@\mathbf{3}$ to the polarization of the π-system of the crown ether's anthracene spacer by the first ammonium ion. This increases positive or diminishes negative partial charges at the second crown ether binding site and thus reduces the binding strength of the second monovalent axle.

To gain further insight into the binding situation, in particular of the illusive complexes composed of the *Z*-configured axles, the Gibbs energies Δ*G* for the 1 : 1 association were calculated by DFT using an approach developed by Grimme.[20] The calculations were performed with TPSS-D3(BJ)/def2-TZVP[21] including solvent effects with the COSMO-RS solvent model.[22] In these calculations it is assumed that one PF_6^- anion is close to the free guest and has to be moved away from the guest during the threading. We have recently described this approach in detail for similar systems and the computed results agree well with the experiment.[23] For *E*-**1**@**3** the calculated Gibbs energy of association Δ*G* (Table S2 in ESI†) is close to the experimental value, validating our method. According to these calculations it turns out that both divalent complexes *Z*-**1**@**3** and *Z*-**2**@**3** are thermodynamically unfavourable. Hence, they should not form in agreement with our experiments showing no evidence for the formation of discrete 1 : 1 complexes in the case of the *Z*-configured axles. Furthermore, the calculations predict a weaker yet favourable interaction energy for *E*-**2**@**3**, which is in line with a weaker π,π-stacking of the more electron-rich stilbene moiety but cannot be compared with experiment since no quantitative data are accessible. The strong stabilisation of the *E*-isomer upon binding to the host is furthermore evident from comparison of the Gibbs energies for the *E*-**1** → *Z*-**1** isomerisation in the free (ΔG = +28.8 kJ mol^{-1}) and in the complexed (ΔG = +115.3 kJ mol^{-1}) form (detailed description see ESI†).

After analysis of the binding of the axles in their two isomeric forms to the host, we were interested in the effect of this complexation on the photoisomerisation behaviour. In the absence of host **3**, axle *E*-**1** shows the typical spectroscopic signature of a regular azobenzene derivative with an intense π,π* band at 333 nm and a weak shoulder at 450 nm associated with the symmetry forbidden n,π* transition (Fig. 3, top). Upon irradiation at 334 nm, the π,π* band decreases while the n–π* band increases and a photostationary state (PSS) with 90% *Z*-**1** is reached. The quantum yield of the $E \rightarrow Z$ photoisomerisation for axle **1** under these conditions is in the expected range $\Phi_{E\rightarrow Z}$ = (6.8 ± 0.1)%. The activation barrier for the thermal $Z \rightarrow E$ isomerisation of *Z*-**1** amounts to $\Delta G^{\ddagger}$ = (110 ± 7) kJ mol^{-1}, giving rise to a thermal half-life of $\tau_{1/2}$ = (127 ± 1) h at room temperature (see ESI†, Fig. S33 and S34). When mixing axle *E*-**1** and host **3**, their absorption spectra largely overlap (for the absorption spectra of individual compounds see Fig. S38 in ESI†). To prevent potential photooxidation of the anthracene moiety,[24] all photochemical experiments were carried out in degassed solvents. Upon irradiation of an equilibrated 1 : 1 mixture of the axle and host compounds at 334 nm, only minor spectral changes were observed, indicating only little photoisomerisation taking place in *E*-**1**@**3**.

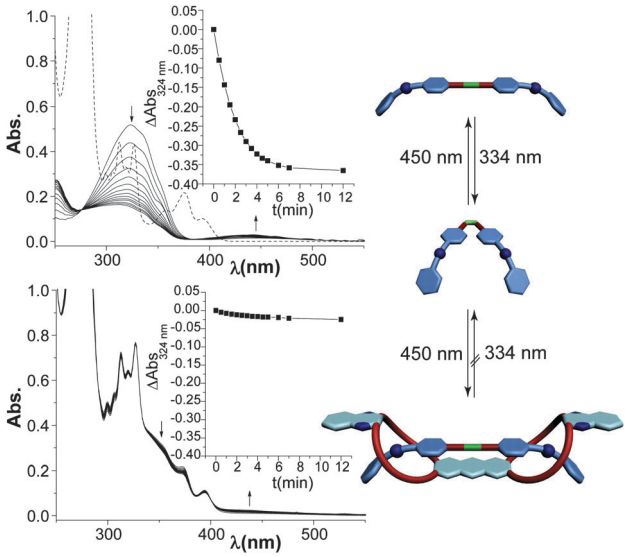

Fig. 3 $E \rightarrow Z$ photoisomerisation of *E*-**1** (40 μM in $CHCl_3$: CH_3CN = 2 : 1) upon irradiation with 334 nm in the absence (top) and presence (bottom) of an equimolar amount of host **3** (dashed line shows spectrum of pure **3**).

This gives evidence for the successful inhibition of azobenzene photochromism (Fig. 3, bottom).

Binding to host **3** selectively inhibits the forward $E \rightarrow Z$ photoisomerisation of **1**, but does not affect the reverse process since irradiation of a PSS mixture (containing 90% *Z*-**1** and 10% *E*-**1**) in the presence of **3** at 436 nm showed clean $Z \rightarrow E$ photoisomerisation (see Fig. S37a in ESI†). However, the presence of host **3** does not accelerate the thermal $Z \rightarrow E$ isomerisation by selective stabilisation of *E*-**1**@**3**, but in contrast the aggregate formed with *Z*-**1** decelerates the thermal back reaction (for comparison of thermal $Z \rightarrow E$ isomerisation in the free and complexed form see Fig. S35, ESI†). However, a clean $E \rightarrow Z$ photoisomerisation can be observed when irradiating *E*-**1** in the presence of excess monovalent host **4**, *i.e.* forming *E*-**1**@$\mathbf{4}_2$ (see Fig. S36b in ESI†). This clearly shows that complexation of the ammonium ions is not responsible for the observed inhibition effect. Furthermore, it is possible to induce $E \rightarrow Z$ photoisomerisation of the dethreaded, unprotonated axle in the presence of **3** (see Fig. S36a in ESI†), showing that the overlapping spectra of both species are neither the reason for the inhibition. Fluorescence measurements (see ESI†, Fig. S39) of the *E*-**1**@**3** complex show no indication of energy transfer at various excitation wavelengths but in contrast, complexation leads to fluorescence quenching of the host, presumably due to photoinduced electron transfer.[25] In view of the strong binding in *E*-**1**@**3** and considering the tuneability of the ammonium ion–crown ether interaction by solvent polarity, another switching experiment was carried out in a more polar solvent mixture, *i.e.* 14 : 1 instead of 1 : 2 CH_3CN : $CHCl_3$. In this case, the attractive interactions between axle *E*-**1** and host **3** are reduced due to competition of their hydrogen bond acceptors and donors with the polar solvent. As a consequence, inhibition becomes much less effective and the photochromic behaviour is recovered (see ESI†, Fig. S37b). Note that the weaker binding under these conditions could not be quantified by ITC due to

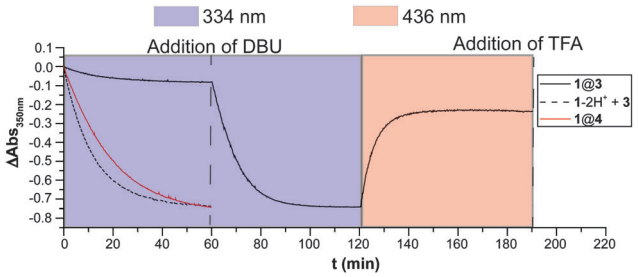

Fig. 4 $E \rightarrow Z$ photoisomerisation of E-**1** in presence of **3** (**1**@**3**, solid black line), deprotonated E-**1** in presence of **3** (**1**–$2H^+$ + **3**, dashed black line), and E-**1** in presence of **4** (**1**@$\mathbf{4}_2$, solid red line) monitoring azobenzene absorption maximum at 350 nm upon irradiation at 334 nm (40 μM in $CHCl_3$: CH_3CN = 2 : 1). After 60 min DBU (4 equiv.) was added to the solution of E-**1**@**3** leading to deprotonation and recovery of photoreactivity. Subsequent $Z \rightarrow E$ photoisomerisation at 436 nm and addition of TFA (4.1 equiv.) reprotonates the axle and resets the system. Note that the system does not recover fully because of the photostationary state of deprotonated **1** and photochemical side reactions of **3**.

insufficient solubility in the acetonitrile-rich medium. All of the above experiments clearly indicate that formation of the E-**1**@**3** complex is actually responsible for inhibition and suggest that in the tight, vice-like pseudo[2]rotaxane binding scenario $E \rightarrow Z$ photoisomerisation is shut down.

Comparing the $E \rightarrow Z$ photoisomerisation at these different conditions, an inhibition efficiency of the pseudo[2]rotaxane system can be estimated. Looking at the decay of the E-azobenzene absorption maximum at 350 nm, one can see that the decrease after 60 min for the complex E-**1**@**3** is approximately 7 times slower than for the deprotonated and therefore non-complexed case, **1**–$2H^+$ + **3**, as well as the monovalent host case, *i.e.* E-**1**@$\mathbf{4}_2$ (Fig. 4, first 60 min). Subsequent *in situ* deprotonation of the binding sites in the E-**1**@**3** complex quickly re-establishes photochromism and results in a fast $E \rightarrow Z$ photoisomerisation. Upon addition of trifluoroacetic acid to the fully converted mixture and irradiating with 436 nm light $Z \rightarrow E$ photoisomerisation takes place and the system is reset thereby showing the reversibility of the process. These experiments demonstrate gating of azobenzene photoisomerisation by addition of either base or acid to the pseudo[2]rotaxane host–guest system.

In the present study, we found a unique way in which strong binding of a divalent azobenzene guest to a complementary host was found to effectively inhibit $E \rightarrow Z$ photoisomerisation. This complexation-induced gating effect can be tuned by changing the strength of the non-covalent interactions, either by varying solvent polarity or more effectively by adding base or acid. On-going work is focusing on shifting the irradiation wavelengths further to the red to achieve a selective excitation of the azobenzene axle.[12]

The authors thank the Deutsche Forschungsgemeinschaft for generous financial support (SFB 765). Support by the High-Performance Computing facilities of the Freie Universität Berlin (ZEDAT) is acknowledged. L.v.K. is grateful to the Studienstiftung des Deutschen Volkes for a PhD fellowship.

Notes and references

1 M.-M. Russew and S. Hecht, *Adv. Mater.*, 2010, **22**, 3348.
2 In a different context this is related to the concept of molecular-scale logic gates, see: A. P. de Silva and N. D. McClenaghan, *Chem. – Eur. J.*, 2004, **10**, 574.
3 J. Zhang, Q. Zhu and H. Tian, *Adv. Mater.*, 2013, **25**, 378.
4 (*a*) T. Hugel, N. B. Holland, A. Cattani, L. Moroder, M. Seitz and H. E. Gaub, *Science*, 2002, **296**, 1103; (*b*) M. Alemani, M. V. Peters, S. Hecht, K.-H. Rieder, F. Moresco and L. Grill, *J. Am. Chem. Soc.*, 2006, **128**, 14446; (*c*) C. Dri, M. V. Peters, J. Schwarz, S. Hecht and L. Grill, *Nat. Nanotechnol.*, 2008, **3**, 649.
5 H. Yu and T. Ikeda, *Adv. Mater.*, 2011, **23**, 2149.
6 (*a*) R. S. Stoll and S. Hecht, *Angew. Chem., Int. Ed.*, 2010, **49**, 5054; (*b*) R. Göstl, A. Senf and S. Hecht, *Chem. Soc. Rev.*, 2014, **43**, 1982.
7 A. Natansohn and P. Rochon, *Chem. Rev.*, 2002, **102**, 4139.
8 (*a*) A. A. Beharry and G. A. Woolley, *Chem. Soc. Rev.*, 2011, **40**, 4422; (*b*) T. Fehrentz, M. Schönberger and D. Trauner, *Angew. Chem., Int. Ed.*, 2011, **50**, 12156; (*c*) T. S. Zatsepin, L. A. Abrosimova, M. V. Monakhova, H. Le Thi, A. Pingoud, E. A. Kubareva and T. S. Oretskaya, *Russ. Chem. Rev.*, 2013, **82**, 942.
9 (*a*) W. Szymanski, J. M. Beierle, H. A. Kistemaker, W. A. Velema and B. L. Feringa, *Chem. Rev.*, 2013, **113**, 6114; (*b*) W. A. Velema, W. Szymanski and B. L. Feringa, *J. Am. Chem. Soc.*, 2014, **136**, 2178.
10 (*a*) X. Chen, L. Hong, X. You, Y. Wang, G. Zou, W. Su and Q. Zhang, *Chem. Commun.*, 2009, 1356; (*b*) G. Wenz, B.-H. Han and A. Müller, *Chem. Rev.*, 2006, **106**, 782; (*c*) D.-H. Qu, Q.-C. Wang, Q.-W. Zhang, X. Ma and H. Tian, *Chem. Rev.*, 2015, DOI: 10.1021/cr5006342; (*d*) S. Yagai, T. Karatsu and A. Kitamura, *Chem. – Eur. J.*, 2005, **11**, 4054; (*e*) S. Hecht, *Small*, 2005, **1**, 26; (*f*) C. Stoffelen, J. Voskuhl, P. Jonkheijm and J. Huskens, *Angew. Chem., Int. Ed.*, 2014, **53**, 3400.
11 (*a*) M. S. Vollmer, T. D. Clark, C. Steinem and R. H. Ghadiri, *Angew. Chem., Int. Ed.*, 1999, **38**, 1598; (*b*) M. Yamamura, Y. Okazaki and T. Nabeshima, *Chem. Commun.*, 2012, **48**, 5724; (*c*) H.-S. Tang, N. Zhu and V. W.-W. Yam, *Organometallics*, 2006, **26**, 22.
12 The thermal half-life of regular (*Z*)-azobenzenes is only on the time scale of minutes to few hours. For a notable recent exception, see: (*a*) D. Bléger, J. Schwarz, A. M. Brouwer and S. Hecht, *J. Am. Chem. Soc.*, 2012, **134**, 20597; (*b*) C. Knie, M. Utecht, F. Zhao, H. Kulla, S. Kovalenko, A. M. Brouwer, P. Saalfrank, S. Hecht and D. Bléger, *Chem. – Eur. J.*, 2014, **20**, 16492.
13 (*a*) J. M. Timko, S. S. Moore, D. M. Walba, P. C. Hiberty and D. J. Cram, *J. Am. Chem. Soc.*, 1977, **99**, 4207; (*b*) P. R. Ashton, P. J. Campbell, P. T. Glink, D. Philp, N. Spencer, J. F. Stoddart, E. J. T. Chrystal, S. Menzer, D. J. Williams and P. A. Tasker, *Angew. Chem., Int. Ed.*, 1995, **34**, 1865; (*c*) W. Jiang, P. C. Mohr, A. Schäfer and C. A. Schalley, *J. Am. Chem. Soc.*, 2010, **132**, 2309.
14 W. Jiang and C. A. Schalley, *Proc. Natl. Acad. Sci. U. S. A.*, 2009, **106**, 10425.
15 M. Linseis, S. Záliš, M. Zabel and R. F. Winter, *J. Am. Chem. Soc.*, 2012, **134**, 16671.
16 T. Bosanac and C. S. Wilcox, *Org. Lett.*, 2004, **6**, 2321.
17 (*a*) W. Jiang, K. Nowosinski, N. L. Löw, E. V. Dzyuba, F. Klautzsch, A. Schäfer, J. Huuskonen, K. Rissanen and C. A. Schalley, *J. Am. Chem. Soc.*, 2011, **134**, 1860; (*b*) L. Kaufmann, N. L. Traulsen, A. Springer, H. V. Schröder, T. Mäkelä, K. Rissanen and C. A. Schalley, *Org. Chem. Front.*, 2014, **1**, 521; (*c*) L. Kaufmann, E. V. Dzyuba, F. Malberg, N. L. Löw, M. Groschke, B. Brusilowskij, J. Huuskonen, K. Rissanen, B. Kirchner and C. A. Schalley, *Org. Biomol. Chem.*, 2012, **10**, 5954.
18 C. A. Hunter, K. R. Lawson, J. Perkins and C. J. Urch, *J. Chem. Soc., Perkin Trans. 2*, 2001, 651.
19 C. A. Hunter and H. L. Anderson, *Angew. Chem., Int. Ed.*, 2009, **48**, 7488.
20 S. Grimme, *Chem. – Eur. J.*, 2012, **18**, 9955.
21 S. Grimme, J. Antony, S. Ehrlich and H. Krieg, *J. Chem. Phys.*, 2010, **132**, 154104.
22 F. Eckert and A. Klamt, *COSMOtherm, Version C3.0, Release 13.01*, COSMOlogic GmbH & Co. KG Leverkusen, Germany, 2013.
23 A. J. Achazi, L. K. S. von Krbek, C. A. Schalley and B. Paulus, *J. Comput. Chem.*, 2015, DOI: 10.1002/jcc.23914.
24 (*a*) E. J. Bowen and D. W. Tanner, *Trans. Faraday Soc.*, 1955, **51**, 475; (*b*) W. Jiang, M. Han, H. Y. Zhang, Z. J. Zhang and Y. Liu, *Chem. – Eur. J.*, 2009, **15**, 9938.
25 M. V. Peters, R. Goddard and S. Hecht, *J. Org. Chem.*, 2006, **71**, 7846.

